



Efficiency of various grouting materials for borehole heat exchangers



Selçuk Erol¹, Bertrand François*

Université Libre de Bruxelles (ULB) Building, Architecture and Town Planning Dept (BATir), Laboratoire de GéoMécanique, Avenue F.D. Roosevelt, 50 – CPI 194/2, B-1050 Bruxelles, Belgium

HIGHLIGHTS

- An admixture is developed with natural graphite flakes for grouting material.
- Thermo-physical, hydraulic and mechanical characteristics are measured.
- The impact on the thermal conductivity is investigated.
- The efficiency of the grout thermal conductivity rises for highly conductive ground.

ARTICLE INFO

Article history:

Received 5 February 2014

Accepted 10 May 2014

Available online 27 May 2014

Keywords:

Ground source heat pump

Grouting material

Graphite

Borehole heat exchanger

Thermal transfer

ABSTRACT

In borehole heat exchangers (BHE), grouting material plays a significant role in the heat transfer between the ground and the heat carrier fluid in the pipes. To guarantee proper sealing capacity of the grouting materials, the grout must also fulfill suitable hydraulic and mechanical properties. This paper evaluates the performance of various grouting materials, through thermal, hydraulic and mechanical laboratory characterizations. In particular, the addition of graphite powder to improve the thermal properties of grouting material is tested. In parallel, the characteristics of two different widely used commercial grouting materials (i.e. bentonite-based and silica sand-based materials) are also investigated. Afterwards, the specific heat exchange rate and the borehole resistance of borehole heat exchangers are assessed experimentally in a $1 \times 1 \times 1 \text{ m}^3$ sandbox under, successively, dry sand and fully water-saturated sand conditions. During the operations, the monitored temperatures in the sandbox are in good agreement with analytical predictions. This study demonstrates that the homemade admixture prepared with 5% natural flake graphite can be considered as an appropriate grout for BHEs regarding to its rheological and thermo-physical properties. Thermally-enhanced grouting can be of significant interest in a high thermal conductivity ground (such as saturated sand) because it minimizes the thermal resistance of the BHE.

© 2014 Elsevier Ltd. All rights reserved.

1. Introduction

Geothermal energy is the form of energy that is extracted from the stored heat ground, and within a range of 0–400 m of depth the stored heat is categorized as shallow geothermal energy. In order to use this energy, there are varieties of different earth-coupled heat extraction systems. The closed-loop geothermal system is one of the mostly used technologies and its configuration comprises a heat exchanger installed inside a borehole and a pump that circulates a solution of water or anti-freeze mixture through the buried

pipes. Thus, the heat is transferred from the ground to the heat carrier fluid.

The ground source heat pump (GSHP) systems for domestic heating and cooling are basically installed in the ground with high density polyethylene (HDPE) pipes and filled the surrounding empty space with grouting material inside the borehole (e.g. in some alternative concepts, groundwater can be used as filling material). In addition to the thermo-physical and hydro-geological conditions of the ground, the characteristics of backfill materials, particularly thermal conductivity, may play an important role for the performance of a borehole heat exchanger.

Most of the commercial grouting materials have a thermal conductivity from 0.8 to $2.4 \text{ W m}^{-1} \text{ K}^{-1}$. Depending on the characteristics of the ground, the considered materials and the geometry of BHE, the specific heat exchange rate is in a range of <20 – 100 W m^{-1} [37].

* Corresponding author. Tel.: +32 2 650 27 35; fax: +32 2 650 27 43.

E-mail addresses: selcuk.erol@ulb.ac.be (S. Erol), bertrand.francois@ulb.ac.be (B. François).

¹ Tel.: +32 2 650 27 46.

Nomenclature

a	thermal diffusivity ($\text{m}^2 \text{s}^{-1}$)
c	specific heat capacity ($\text{J kg}^{-1} \text{K}^{-1}$)
L	borehole length (m)
R_b	unit length borehole resistance including pipe resistance (K m W^{-1})
R'_b	unit length borehole resistance excluding pipe resistance (K m W^{-1})
r_i	inner radius of pipe (m)
r_o	outer radius of pipe (m)
r_b	radius of borehole (m)
q	specific heat exchange rate per unit length of borehole obtained theoretically (W m^{-1})
Q_1	heat flow rate (J s^{-1})
Q	specific heat exchange rate per unit length of borehole obtained experimentally (W m^{-1})
t	time (s)
T	temperature ($^{\circ}\text{C}$)
V	volumetric flow rate of fluid inside the pipes ($\text{m}^3 \text{s}^{-1}$)
x, y, z	space coordinates (m)
xc	half shank distance (m)

Greek symbols

λ	thermal conductivity ($\text{W m}^{-1} \text{K}^{-1}$)
ρ	density (kg m^{-3})
ψ	heat transfer rate ($\text{W m}^{-2} \text{K}^{-1}$)

Subscripts

F	fluid
-----	-------

Jun et al., [21] analyzed with the analytical line source model the effect of the thermal conductivity of grout mix on both the thermal resistance and heat exchange rate. For this study, they determined the range of grout thermal conductivity from 0.75 to $2.4 \text{ W m}^{-1} \text{K}^{-1}$, and with increasing the thermal conductivity of grout, the thermal resistance is reduced and the heat exchange rate is increased. They recommend that the thermal conductivity of grout mix should be larger than the ground thermal conductivity in the absence of groundwater flow. Desmedt et al. [8] investigated experimentally the performance of BHEs with different grout materials. They concluded that the addition of sand to the cement-bentonite based grout mix increase the performance of system, but they did not observe that the thermally enhanced grout mix improves the performance of the GSHP system compared with a low-cost grouting material. Borinaga-Treviño et al., [5] performed 4 thermal response tests (TRT) in similar geological area and each borehole is filled with different grout mix. They demonstrated that the thermal resistance of grout mix is reduced with increasing thermal conductivity of grout.

In order to improve the specific heat exchange rate of BHEs, thermal conductivity of the grouting material can be enhanced. Remund & Lund [30] showed that the thermal conductivity of bentonite-based grout is relatively low and is needed to be mixed with thermally enhanced material such as sand to improve the thermal conduction between the pipes and surrounding ground. Allan & Philippacopoulos [2] studied on the thermal, mechanical and hydraulic properties of grout materials. They developed a grout mix (MIX 111) enhanced with silica-sand that has a thermal conductivity up to three times higher than bentonite-based grout. In the last decade, particularly graphite-based admixtures have been investigated to enhance the thermal conductivity of grouting

material. Jobmann et al., [20] studied on the influence of graphite addition on the grouting material as a sealing of heat-generating radioactive waste. They reached an enhanced thermal conductivity of approximately $3 \text{ W m}^{-1} \text{K}^{-1}$ with 14% water content and 15% graphite. Lee et al., [23] indicated that with increasing the content of silica-sand and graphite in an admixture, the thermal conductivity value rises, but the viscosity of the admixture also increases. As a result, by adding 30% graphite to bentonite-based admixture led to a thermal conductivity of $3.5 \text{ W m}^{-1} \text{K}^{-1}$. In addition Lee et al., [24], developed an admixture containing cement, silica-sand and graphite providing a thermal conductivity of $2.6 \text{ W m}^{-1} \text{K}^{-1}$ that they experienced through in-situ thermal response tests (TRT). Recently Delaleux et al., [7], claimed that by adding less than 15% graphite powder in an admixture, thermal conductivity of $5 \text{ W m}^{-1} \text{K}^{-1}$ can be reached. Nevertheless, in most of those previous works, other necessary parameters such as permeability, compression strength and workability, were not determined to proof the applicability of those admixtures as a grouting material. Good sealing capacity of the grouting materials (needed to provide a watertight closure of the borehole to minimize the environmental impacts) requires a sufficiently low permeability and a good strength to avoid failure upon thermal stress. Good workability at fresh state is needed to guarantee the pumpability of the mixture during the pouring of the grout in the borehole.

The main objective of the present research being to evaluate the suitability of various grouting materials for BHE, the focus is made, not only on the thermal improvement, but also on the other rheological properties of the grout in order to guarantee a proper behavior of the BHE. The aim of the present study is to validate that the admixtures prepared with different types of graphite powder can be used as a backfilling material for BHEs. The study is carried out through a three-step approach:

- First, thermal, hydraulic and mechanical laboratory tests have been performed to determine the suitability of grouting materials for BHE. The characteristics of different homemade and commercial grout mix materials are evaluated in laboratory under fresh and solid state. This step allows us to leave aside some of the grout mixtures due to their unsuitable properties (strength, permeability, flowability).
- Then a small-scale sandbox TRT has been operated for two different commercial products (bentonite-based and silica sand-based materials) and one homemade admixture containing natural flake graphite. The performance of selected grout mix materials are compared with two different thermo-physical soil conditions (under dry (solid-air) sand and under fully water-saturated sand).
- Finally, sandbox tests have been reproduced by analytical studies to evaluate the specific heat exchange rate and the thermal resistance of BHE. Analytical models being well known solutions, our purpose is not to verify the solution, but rather to use it to validate the properties of the grout mix (to check that the temperature field generated by the operation of BHE is in agreement with the expected properties of the BHE).

2. Admixtures

2.1. Commercial grouting materials

In order to investigate the range of specific heat exchange rate depending on the typical characteristics of grouting materials, first analyses are carried out by considering two different commercial products known as suitable materials for backfilling BHEs. One of the considered products is bentonite-based having the lowest

thermal conductivity and other is thermally enhanced silica sand-based grout mix. Those two products have been chosen for their relatively high difference in thermal conductivity, in order to have a large range of variation. The objective is to justify how the grouting materials drive the heat exchange rate.

Although, the important characteristics of commercial products such as permeability, thermal conductivity, density, etc. are already provided by the producers, these parameters are determined in the laboratory to compare with the experiment results of the home-made admixtures.

2.2. Homemade admixtures

The considered graphite types for the pre-analyses (i.e. mechanical and thermo-physical tests) are listed by increasing cost: (1) natural flake graphite (TIMREX M 100/45–150 μm), (2) the primary synthetic graphite with two different grain size distributions (TIMREX KS 150/150 μm , TIMREX KS 150–600/150–600 μm), and (3) expanded graphite powder (TIMREX C-THERM 011/2.5% ashes) [36]. The components are mixed with various ranges (5–12% graphite, 24–40% silica sand (D 50 = 260 μm), 24–45% water, 20–28% cement and 0–7% Ca^{2+} bentonite), in order to determine the fraction contents of admixtures. According to the preliminary (visual) observations, and also regarding to the guidelines VDI 4640 (Blatt – 2 & 3) and [1,2]; the proportion of graphite shall be less than 10% and silica sand should not exceed 50%, because graphite absorbs large amount of water and with the addition of silica sand the pumpability of admixture becomes unfeasible due to its high viscosity [38]. Therefore, the amount of graphite powder is kept 5% in all prepared homemade admixtures.

3. Laboratory characterization of grout materials

The major authorities for planning the GSHP systems such as VDI 4640 from Germany, ASHRAE from USA and BS institution from UK present guidelines concerning the proper installation methods, optimum geometry design of BHEs, and particularly, rheological properties of sealing materials. The principal tasks about the grouting materials are to provide a good thermal conduction between the pipes and surrounding ground and to ensure a water-tight, durable and frost-proof material [18,31]. Even if the main objective of the grouting material is to maximize thermal transfer, the grout must have specific hydraulic and mechanical properties in order to ensure a good sealing of the borehole. However, the guidelines provide only suggestions about the backfilling materials referring to the environmental criteria and the performance optimization of the system, but the standards of grout mix material for a BHE adapted as a function of the ground conditions are elusive on the other expected rheological parameters. Therefore, in order to propose an appropriate grouting material, the characteristics of grouting materials are determined with the standard methods specified for soil, rock and concrete and the measured values of parameters are compared with the values of well-known commercial materials and also in accordance with guidelines.

3.1. Permeability

The low permeability of grouting material is an important property to avoid interaction between the pipes and surrounding ground (in case of leakage of circulating anti-freeze inside the pipes) or to limit the inter-connection between independent overlying aquifers. A standard test method, the falling head permeameter ASTM D 5084 – 90, has been used to determine the permeability. This method is well-adopted for low permeability

materials, as it is expected for the grout. The allowable permeability of backfilling material shall be $\leq 1 \times 10^{-9} \text{ m s}^{-1}$ [14].

One silica sand-based sample and four bentonite-based grout samples having different fraction of water are prepared (i.e. water/bentonite ratio $w/b = 0.5, 0.6, 0.7, 0.8$).

The considered grouting materials are placed inside the cells, when they are fresh. Then the samples are left for curing for one day under water. Then the falling hydraulic head in the pipe is measured through 30 days to calculate the permeability. Thereby, the permeability can be evaluated as a function of curing time.

3.2. Uni-axial compression strength

During the operation of the BHE, the grouts may be subjected to significant variation of stress state due to various effects (mainly related to thermal and/or freezing stresses). Failure of the grouting material upon those stress variations would jeopardize the water tightness and the sealing capacity of the grout. It explains why a minimum strength should be satisfied. However, there is no criterion defined in the norms for the strength of grouting materials. The comparison is carried out with the provided values of commercial materials.

The scope of the uniaxial compression test is to determine the compression strength of a grouting material with unrestricted horizontal deformation. The DIN 18 – 136 is followed to conduct the experiment using a displacement-controlled loading frame, in order to be able to catch the post-peak response of the material.

Before compression tests, the prepared fresh samples are placed in a humidity room (~80% humidity) under constant temperature at 20 °C, and curing time is set to 10 days and 30 days to observe how the strength of the materials changes in time.

3.3. Thermal conductivity

Thermal conductivity of grouting material is determined according to the ASTM D 5334 – 08 with a thermal needle probe device TP02 produced by Hukseflux company (1.5 mm diameter and 150 mm length). In fact, this standard method is conducted for measuring the thermal conductivity of soil and soft rock, but since there is not a specified method to determine the thermal conductivity of grout mix, we constructed our own setup with the thermal needle probe to estimate the thermal conductivity of grout mixtures. To validate our methodology, the thermal conductivity of commercial materials are determined in laboratory and compared with the values provided by the producers.

The electrical resistance of the heating wire, which is the 2/3 of the needle length, is 75.43 Ohm m^{-1} , and the applied current is 277 mA. The voltage is recorded as an output signal through a testing time of approximately 200 s, and the measured data are evaluated and plotted as the slope of $4\pi\Delta T/Q_T (\text{m K W}^{-1})$ versus $\ln(t)$, where Q_T is the heating power per unit length. The most linear part of the regression curve is determined to estimate the thermal conductivity [25].

While the admixture material is fresh, a thin rigid stick that has the same diameter than the needle probe (1.5 mm) is placed in the middle of sample (cylinder shaped sample $d = 100 \text{ mm}$, $h = 200 \text{ mm}$). Thereby, the rigid stick can be replaced by the needle probe into the sample when it is dried. During the thermal conductivity measurement, the surrounded gap between the sample and the needle is filled with a highly-conductive thermal paste ($\lambda_{\text{paste}} \sim 8 \text{ W m}^{-1} \text{ K}^{-1}$) to avoid artifacts due to air included in the gap.

3.4. Workability

The workability of fresh admixture depends on the water content and the shape and size distribution of the components and

plays a major role on the pumping process of the grouting material during the installation. In existing norms for grout mix, it is only suggested to avoid high silica sand fraction in the mixture due to difficulties during the injection of grout to the borehole. Therefore, our aim to conduct this method is to classify different grout mixtures with its flowability and plastic viscosity. For determining the pumpability and the plastic viscosity of admixtures, the flow cone method, so called Marsh cone, (ASTM – C 939 94a) is performed.

The specified volume of fresh grout, 1725 mL, flows through the nozzle of the cone, and the time of efflux of suspension is measured in seconds. An empirical method is described by Ref. [32] to classify the flowability of different suspensions. The represented criterion is related to several rheological parameters (i.e. plastic viscosity and yield stress) which can be calculated depending on the efflux time, density of grout and cone geometry (e.g. height of the cone, radius of the nozzle).

4. Small-scale BHE characterization

4.1. The sandbox experiment

The sandbox experiment consists in the operation of a BHE of 1 m in length installed in an insulated box of $1 \times 1 \times 1 \text{ m}^3$ filled by sand. The BHE includes two parallel pipes in HDPE which are operated with two heat pumps that circulate water with temperature fixed at 12°C (inlet) and at 15°C (outlet), respectively (Fig. 1) while the initial temperature was fixed at 20°C . Table 1 reports the dimensions and characteristics of the sandbox and BHEs.

The objective of the test is to investigate, from an experimental point of view, the impact of the thermal conductivities of grouting and ground on the heat exchange rate and borehole resistance. Then, the obtained values are compared with theoretical predictions. To that purpose, three different grouting materials have been experienced: two commercial products (C-1 silica sand-based and C-2 bentonite-based) and one homemade admixture (A-2 containing natural graphite). The three BHE probes are operated under dry sand (air-solid) and fully water-saturated sand. Consequently, six tests have been performed. Thermal properties of the different materials in the sand box are reported in Table 2.

Table 1

Dimensions and characteristics of the sandbox and borehole heat exchanger.

Parameters		Value
Radius of BHE	r_b	0.068 m
Length of BHE	L	1 m
Outer radius of the pipe	r_o	0.016 m
Inner radius of the pipe	r_i	0.0131 m
Pipe distances (Center to center)	$2x_c$	0.083 m
Volumetric flow rate inside the pipes (Turbulent flow with the Reynold number of 1.1×10^4)	V	$3.66 \times 10^{-4} \text{ m}^3 \text{ s}^{-1}$
Initial temperature of sandbox	T_0	20°C

In a real operation, the pump circulates the fluid through the geothermal probe ($\sim 100\text{--}200 \text{ m}$) to have a thermal gradient between inlet and outlet by the heat exchange with the ground. In the present test, the 1 m probe length is not enough to produce a significant temperature difference between inlet and outlet that is approximately 3°C . Therefore, the fluid temperatures in the two pipes are controlled separately. The widely used method to estimate the specific heat exchange rate of a BHE, based on the temperature difference between inlet and outlet, is not applicable in our case due to the considerably small difference of temperature between inflow and outflow of each pipe ($<0.1^\circ\text{C}$ with a BHE of 1 m in length) with regards to the sensor accuracy ($\pm 0.03^\circ\text{C}$) and the resolution of the acquisition device ($\pm 0.1^\circ\text{C}$). As described in Section 4.2.2, backward computations based on analytical solutions of temperature evolution in the sand is used to deduce to the specific heat exchange rate.

The walls of the sandbox and the pipes from the probe to the heat pumps are well isolated. The operation time is set to the minimum suggested duration of a TRT, 50 h [3,13], to avoid as much as possible the influence of ambient temperature on the temperature distribution inside the sandbox. Also after 50 h, the radius of influence of the BHE reaches the wall of the box.

Since the temperature distribution is symmetric in the sandbox due to conduction dominated heat transfer system, the temperatures are measured along one radial axis of BHE with pt-100 precision thermistors. Additionally, two thermistors are placed inside

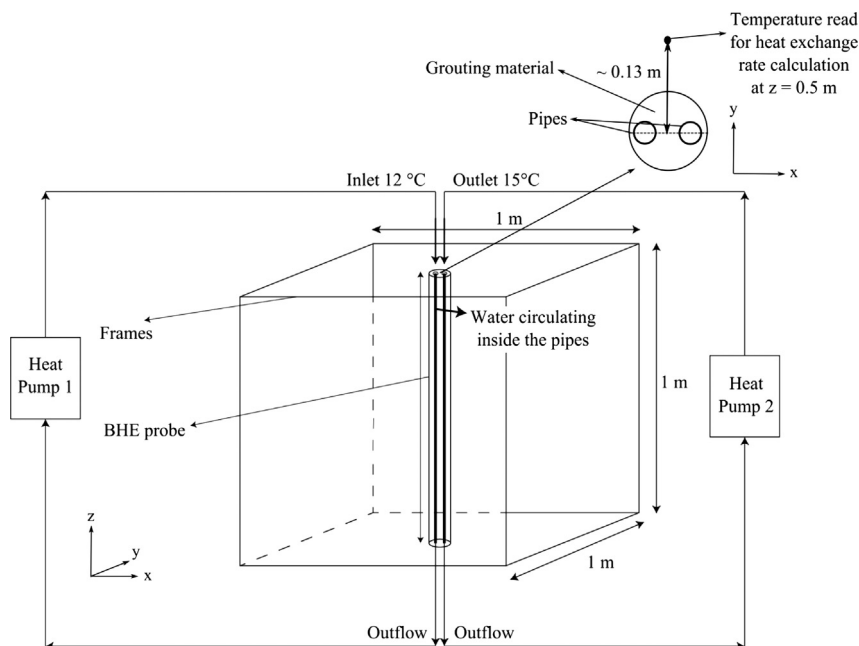


Fig. 1. Scheme of the sandbox TRT operated with two separated heat pumps.

Table 2
Thermal characteristics of the pipe, water, air and silica sand.

Parameters	Thermal conductivity [W m ⁻¹ K ⁻¹]	Bulk volumetric heat capacity [MJ m ⁻³ K ⁻¹]
Pipe ^a	0.42	2.08
Silica sand (air – solid) ^c	0.35 ^d	1.23 ^b
Silica sand (water-saturated) ^c	2.3 ^d	3 ^b

^a [15].

^b [39].

^c Bulk thermal properties of sand with the porosity of 0.43 [–] [34].

^d measured value.

the pipes where the fluid flows into the BHE, to correct the temperature difference between the heat pump and the probe.

4.2. Analytical solution

In this study, the objective of analytical solution is twofold. First, it allows us to calculate theoretically the borehole resistance, the heat exchange rate and the temperature distribution around the BHE, as a function of thermal characteristics of the grout and of the ground. Those theoretical predictions can be therefore compared with experimental measurements, in order to demonstrate that the thermal properties as determined in laboratory are effective in the condition of the BHE. Secondly, the analytical solution provides a way to deduce the heat exchange rate of the BHE through back-analysis of the temperature distribution in the ground. In the following those two objectives are successively described.

Analytical solutions for BHEs consider mostly conduction dominated systems [6,19], and a few studies take into account the axial effect [11,26,41] or the groundwater flow effect in the underground [9,35], Molina-Giraldo et al., 2011 [27], [40,10]. However, those assumptions consider a constant heat load to calculate the temperature change in the surrounding ground. Since the mean fluid temperature is fixed to a certain value, the heat input changes as a function of time.

4.2.1. Analytical predictions

First, the time-dependent heat exchange rate per unit length of BHE can be obtained as a function of the mean fluid temperature by taking line source method derived by Ref. [6] and adding the effective borehole resistance [12]:

$$q(t) = \frac{(T_0 - T_f)}{\left[\frac{1}{4\pi\lambda_{soil}} E_1 \left(\frac{r_b^2}{4at} \right) + R_b \right]} \quad (1)$$

where a is the thermal diffusivity of soil, T_0 is the undisturbed soil temperature. $E_1(r_b^2/4at)$ is the exponential integral function of $r_b^2/4at$ that has been solved through a MATLAB function.

This equation requires the estimation of the borehole resistances that can be analytically obtained regarding to the geometry and the thermal characteristics of the BHE. It accounts for the convection and conduction pipe resistances and effective borehole wall resistance [22]:

$$R_b = \underbrace{R'_{conv} + R'_{cond}}_{R_{pipe}} + R'_b \quad (2)$$

As illustrated in Fig. 2, the total borehole thermal resistance includes pipe resistance R_{pipe} (decomposed into convection and conduction resistance R'_{conv} and R'_{cond} , respectively) and grout thermal resistance R'_b . The two pipe resistances are given as follows:

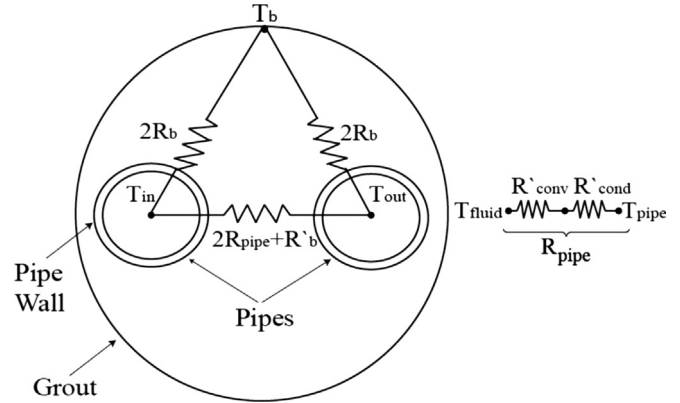


Fig. 2. Scheme of a single U-shaped pipe BHE thermal resistances (After Lamarche et al., 2010).

$$R'_{conv} = \frac{1}{4\pi r_i \psi} \quad (3)$$

$$\psi = \frac{Nu \lambda_f}{2r_i} \quad (4)$$

$$R'_{cond} = \frac{\ln(r_o/r_i)}{4\pi\lambda_{pipe}} \quad (5)$$

in which r_i and r_o are the inner and outer radius of pipes, respectively. ψ is the heat transfer coefficient estimated with Nusselt number (Nu), inner radius of the pipe r_i and thermal conductivity of the fluid λ_f .

The third contribution of Eq. (2) is a 2D grout thermal resistance that can be obtained analytically by different methods [16,29,33]. In particular [4], used the multipole method. Lamarche et al., [22] shows that, among other approaches under steady-state and transient conditions, the multipole solution provided the best estimation with regard to the numerical results. For single U-shaped pipe, the first-order solution is given as follows:

$$R'_b = \frac{1}{4\pi\lambda_{grout}} \left[\ln \left(\frac{\alpha_1 \alpha_2^{1+4\eta}}{2(\alpha_2^4 - 1)^\eta} \right) - \frac{\alpha_3^2 \left(1 - \frac{4\eta}{(\alpha_2^4 - 1)} \right)^2}{1 + \alpha_3^2 \left(1 + \frac{16\eta}{((\alpha_2^4 - 1)/\alpha_2^2)^2} \right)} \right] \quad (6)$$

in which α_1 , α_2 , α_3 and η are the dimensionless parameters and given as follows:

$$\eta = \frac{\lambda_{grout} - \lambda_{soil}}{\lambda_{grout} + \lambda_{soil}} \quad (7)$$

$$\alpha_1 = \frac{r_b}{r_o} \quad (8)$$

$$\alpha_2 = \frac{r_b}{x_c} \quad (9)$$

$$\alpha_3 = \frac{r_o}{2x_c} \quad (10)$$

where r_b is the radius of borehole, r_o is the outer radius of pipe and x_c is the half shank spacing (the distance from the center of the pipe to center of BHE).

In the last step, the calculated heat input rate Eq. (1) as a function of time can be taken into account in order to evaluate the time-dependent temperature distribution in the ground around the BHE.

The analytical solution of heat transfer for a continuous point source in an infinite porous medium is given by Ref. [6]:

$$\Delta T(x, y, z, t) = \frac{Q_1}{4\pi\lambda_{soil}D} \operatorname{erfc}\left[\frac{D}{\sqrt{4at}}\right] \quad (11)$$

where Q_1 is the heat flow rate and D is the distance to the source point in 3D Euclidean space and expressed as:

$$D = \sqrt{x^2 + y^2 + z^2} \quad (12)$$

The Eq. (11) yields the finite line source solution (Eq. (13)) by applying the method of images [41].

$$\Delta T(x, y, z, t) = \frac{q(t)}{4\pi\lambda_{soil}} \left[\int_0^L \frac{1}{D'} \operatorname{erfc}\frac{D'}{\sqrt{4at}} dz' - \int_{-L}^0 \frac{1}{D'} \operatorname{erfc}\frac{D'}{\sqrt{4at}} dz' \right] \quad (13)$$

where L is the length of BHE and D' is the distance to the source placed at a depth z' on the z axis in 3D Euclidean space given as:

$$D' = \sqrt{x^2 + y^2 + (z - z')^2} \quad (14)$$

As the assumption of Eq. (13), the line source extends from the top boundary to a certain depth L . Temperature of the top boundary is kept constant and vertical (axial) heat flux is taken into account at the bottom of the line source. Let's note that the boundary condition of the sandbox is slightly different but the temperature measurements being taken at mid-depth of the box, the boundary conditions play insignificant role.

4.2.2. Experimental evaluations

In addition to the theoretical predictions of borehole resistance and heat exchange rate, as described in the previous section, those two characteristics can be measured during the operation of the BHE in the sandbox.

First, the borehole resistance can be evaluated according to its traditional definition [17]:

$$R_b = \frac{T_f(t) - T_b(r_b, t)}{Q(t)} \quad (15)$$

where T_f and T_b are the mean fluid temperature and the borehole wall temperature, and $Q(t)$ denotes the specific heat exchange rate per unit length of borehole that must be deduced. T_b is obtained at ($x = 0$ m, $y = 0.068$ m, $z = 0.5$ m).

Knowing the experimental temperature distribution, Eq. (13) can be solved backward to deduce the specific heat exchange rate. One of the temperature measurement in the sandbox at where the temperature distribution is symmetric can be taken into account for $\Delta T_{ex}(x, y, z, t)$ to calculate $Q(t)$. In practice, the temperature at ($x = 0$ m, $y = 0.13$ m, $z = 0.5$ m) have been considered.

$$Q(t) = \frac{4\pi\lambda_{soil}\Delta T_{ex}(x, y, z, t)}{\left[\int_0^L \frac{1}{D'} \operatorname{erfc}\frac{D'}{\sqrt{4at}} dz' - \int_{-L}^0 \frac{1}{D'} \operatorname{erfc}\frac{D'}{\sqrt{4at}} dz' \right]} \quad (16)$$

5. Results

5.1. Laboratory test results

The test results are basically compared between two commercial grouts used for BHE installations and homemade admixtures. Some primary observation results about different types of grouting materials are expressed as follows:

- During the curing period of fresh grouts, the samples are extremely fragile for first 2 or 3 days.
- All samples cured under high humidity or under water do not show any visible crack or shrinkage on its diameter. On the other hand, under dry room temperature conditions some fractures and shrinkage are observed only on the bentonite-based grout.
- High water fraction (more than its saturation) in an admixture causes air bubbles.

The fundamental comparison of all variant results can be found in Table 3. As the reference measurement, the results of two commercial products are nearly in agreement with the values provided by the producers.

Comparing the results of homemade grouts with the reference values of the commercial grouts, permeability, density and compression strength results are in an allowable range, except the

Table 3
Measured parameters for two commercial grouting materials and homemade admixtures.

Admixtures	Permeability [m s ⁻¹]	Density [kg m ⁻³] × 10 ³	Plastic viscosity [Pa s]	Marsh cone‡ [s/1725 mL]	Compression strength [N mm ⁻²]	Thermal conductivity [W m ⁻¹ K ⁻¹]
C-1 silica sand-based	<1 × 10 ⁻⁹ #/6 × 10 ^{-10*}	~1.8#/~1.8**	–	No flow	10# /9.3**/3.8‡	2.35# /2.3**
C-2 bentonite-based w/b = 0.5	<1 × 10 ⁻¹⁰ # /4.3 × 10 ^{-12*}	~1.7**	–	No flow	–	–
C-2 bentonite-based w/b = 0.6	<1 × 10 ⁻¹⁰ #/9 × 10 ^{-12*}	1.66# /~1.66**	~0.20	25 ± 1	8.5#/8.7** /3.1‡	0.95# /0.9**
C-2 bentonite-based w/b = 0.7	<1 × 10 ⁻¹⁰ #/8.1 × 10 ^{-11*}	1.6#/~1.6**	~0.13	17 ± 1	–	–
C-2 bentonite-based w/b = 0.8	<1 × 10 ⁻¹⁰ #/2.8 × 10 ^{-10*}	1.55#/~1.54**	~0.11	14 ± 1	–	–
A-1 without graphite	2.8 × 10 ^{-12*}	~1.75**	~0.23	27 ± 1	8.2**	1.5**
A-2 with natural graphite	4.4 × 10 ^{-12*}	~1.7**	~0.6	72 ± 1	8**	2.3**
A-3 with synth. graphite 150 μm	2.2 × 10 ^{-12*}	~1.75**	~0.41	48 ± 1	10**	2.5**
A-4 with synthetic graphite 150–600 μm	3.3 × 10 ^{-12*}	~1.75**	~0.19	22 ± 1	9.8**	1.9**
A-5 with expanded graphite	>1 × 10 ^{-3*}	~1.2**	~0.36	61 ± 1	1.7**	2.3**

*Measured values after the curing period of 45 days (cured under water), ** and ‡ Values are the average of two samples and measured values after the curing period of 30 days and 10 days, respectively (cured under 80% humidity at constant temperature 20 °C), # values provided by producers, § backward calculations based on efflux time, density and the properties of Marsh cone geometry [32], † radius of nozzle 5 mm, cone angle tan(α) = 0.253.

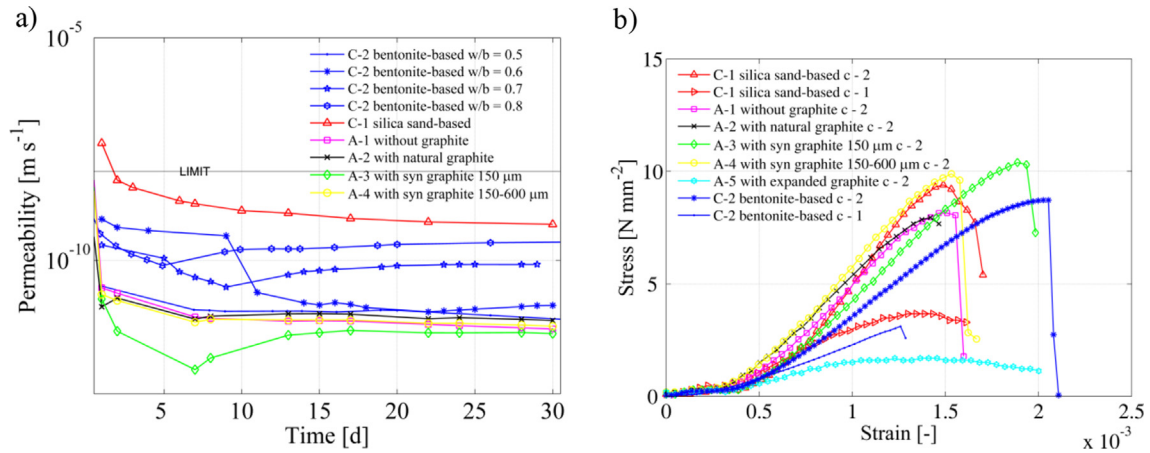


Fig. 3. Comparison results between different types of admixtures a) permeability b) compression strength results. w/b ratio of bentonite-based grout is 0.6. c – 1 presents the curing period of 10 days and c – 2 denotes 30 days.

result of admixture prepared with expanded graphite A-5 for which permeability $\leq 1 \times 10^{-9}$ m/s is not fulfilled, and the lowest compression strength and density is observed among other grouts. The reason is that the expanded graphite has lower density than the other graphite powders (e.g. expanded graphite bulk density = 150 kg m⁻³, synthetic graphite 150–600 μ m bulk density = 670 kg m⁻³).

The higher fraction of sand in A-1 (40%) and the larger size graphite grains (>300 μ m) which are sunk into the bottom of A-4 sample caused the sedimentation in those admixtures. Except the

admixtures A-1 and A-4, other suspensions are mixed homogeneously.

As far as the Marsh cone test results are concerned, the flowability of A-1 and A-4 admixtures are considerably higher than other homemade grouts, because the well-graded grain size distribution decreased both the yield stress and the plastic viscosity of those suspensions. On the other hand, the efflux of silica sand-based grout and C-2 bentonite-based w/b = 0.5 is stopped in the Marsh cone after several drops, even if they are homogeneous mixtures. The efflux time of bentonite-based grouts is decreasing

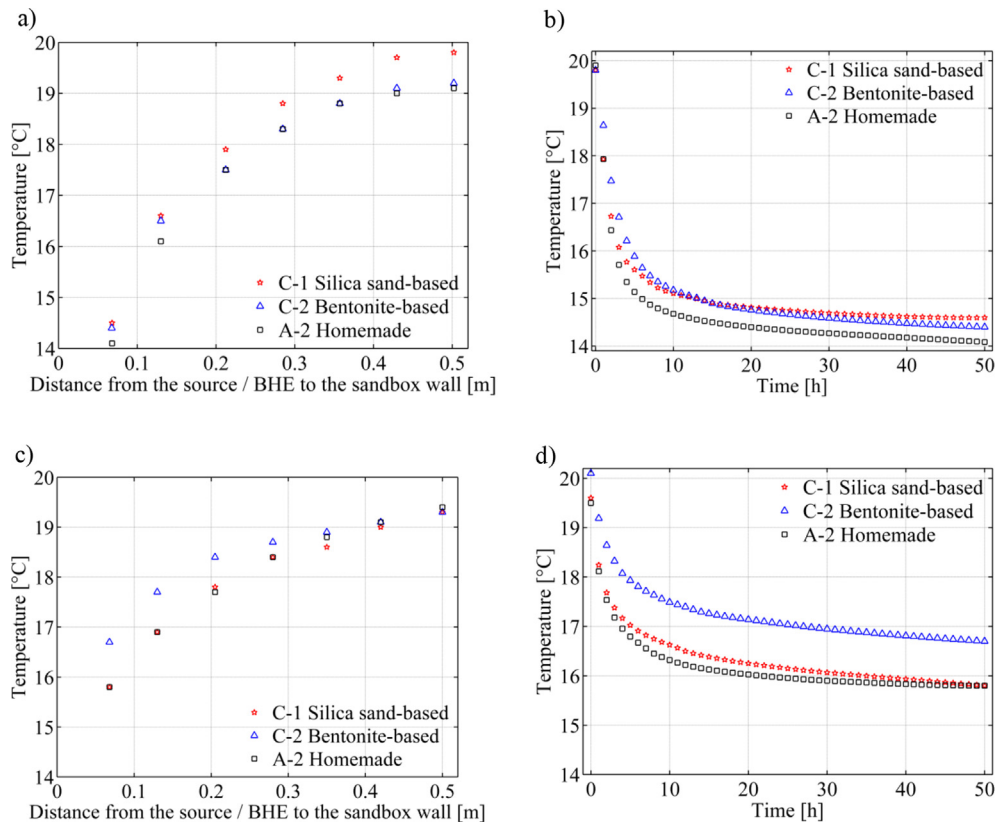


Fig. 4. Comparison of experimental measurement: a) and b) dry sand (air – solid); c) and d) under water-saturated sand. a) and c) at 50th operation hour ($x = 0$ m, $y = 0.068$ m – 0.5 m, $z = 0.5$ m); b) and d) over time ($x = 0$, $y = 0.068$ m, $z = 0.5$ m).

with rising w/b ratio due to decreasing viscosity. The calculated plastic viscosity results are proportional to the efflux time of all admixtures and vary depending on the component characteristics of grouts (e.g. grain size distribution of components). According to the results, the bentonite-based C-2 commercial material with $w/b \geq 0.6$ is more convenient to pump for installation of a BHE regarding to other admixtures.

The thermal conductivity results of homemade admixtures demonstrate that 5% addition of graphite has a significant impact on the thermal conductivity of grout (e.g. A-1 without graphite = $1.5 \text{ W m}^{-1} \text{ K}^{-1}$, A-2 with natural graphite = $2.3 \text{ W m}^{-1} \text{ K}^{-1}$). Compared to the results between A-2 to A-5, different type of graphite powders do not alter considerably the thermal conductivity, likely, due to its smaller fraction in the admixture.

In Fig. 3a), C-1 silica sand-based grout gives the highest permeability compared to bentonite-based and homemade samples. It is mainly explained by the larger grain size distribution of C-1 than other grouts. On the other hand, the permeability of bentonite-based grout varies with rising w/b ratio, because the high water saturation of admixture causes low suspension density and, therefore, an increase of infiltration rate. A-5 homemade admixture is not shown in the figure due to its very high permeability ($>1 \times 10^{-3} \text{ m/s}$) (Table 3). Generally, the coefficient of permeability of the grouting material decreases with curing time. The cured grout (after 30 days) has a lower permeability than the fresh grout (after 1 day).

In Fig. 3b), after a flat first part of the curve (corresponding to the closure of the gap between the loading piston and the sample), uniaxial compression curves give a straight line that demonstrates the elastic behavior of the grouts. Then, under high load, non-linear curve shows plastic behavior. The compression strength of each material is taken as the peak value of each curve. When C-2 bentonite-based grouts reach its elastic limit, then a sudden failure occurs that is the characteristic of brittle response. On the contrary, C-1 silica sand-based grout exhibits plastic hardening behavior, when the stress exceeds its elastic limit. After the peak point, C-1 silica sand-based grout fractured. The results of homemade admixtures (A-1 to A-5) provide nearly identical elastic behavior, except the admixture A-5. Obviously, the density and the texture of expanded graphite have a negative impact on the mechanical behavior (in terms of stiffness and ultimate strength).

Concerning the curing period of samples (only for commercial grouts), the samples performed for the test after 10 days (c – 1) fractured under lower axial stress than other samples cured for 30 days (c – 2). According to the results, it is not appropriate to start an operation of BHE earlier than 30 days of curing after the installation due to brittleness of the grouting material.

5.2. Sandbox experiment results

Fig. 4 shows the comparison of the experimental temperature results obtained with different grout materials under dry sand (Fig. 4a) and b) and water-saturated sand conditions (Fig. 4c) and

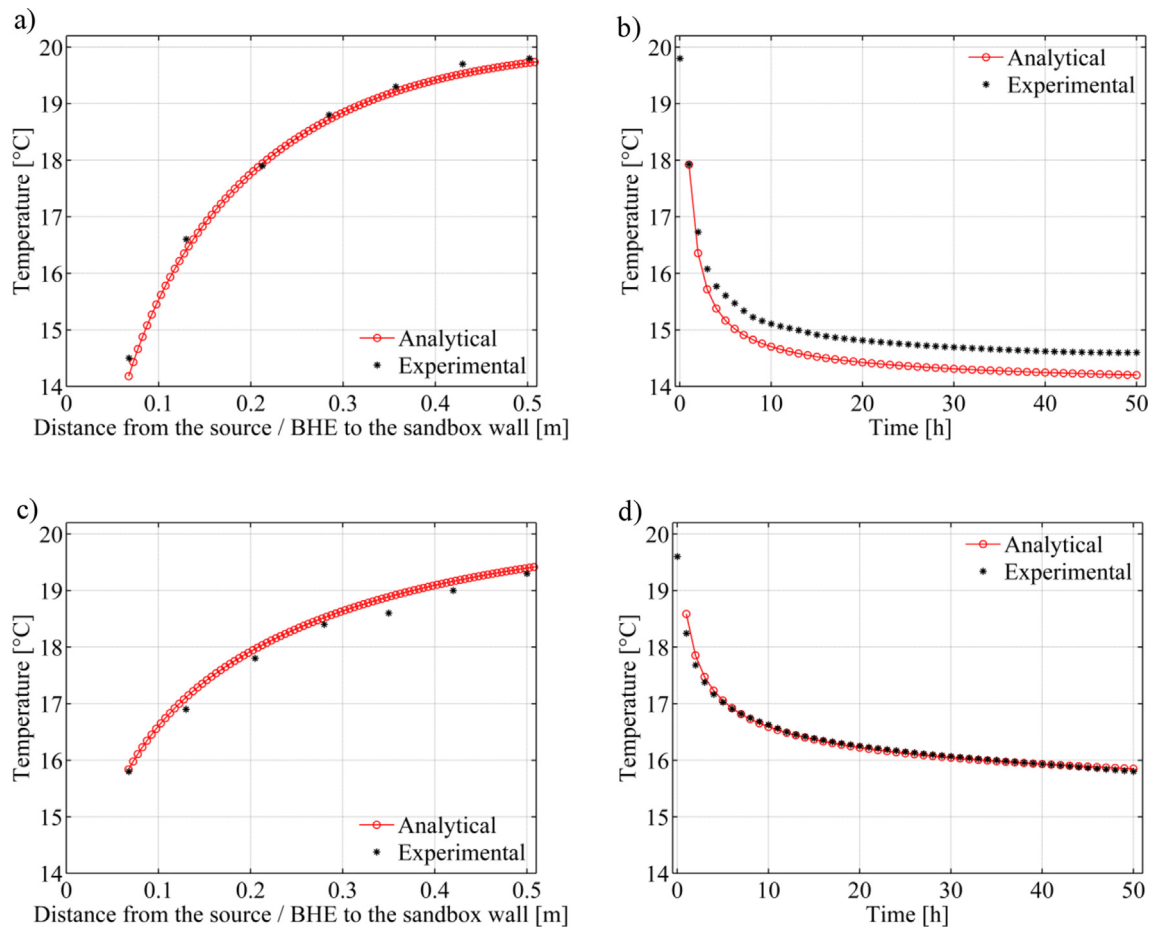


Fig. 5. Comparison of experimental measurement with analytical (Eq. (13)) solution for BHE probe prepared with C-1 silica sand-based grouting: a) and b) dry sand; c) and d) under water-saturated sand. a) and c) at 50th operation hour ($x = 0 \text{ m}$, $y = 0.068 \text{ m}$ – 0.5 m , $z = 0.5 \text{ m}$); b) and d) over time ($x = 0$, $y = 0.068 \text{ m}$, $z = 0.5 \text{ m}$).

d)). In Fig. 4a), the influence of room temperature on the sandbox wall can be seen, particularly, on the results of C-2 and A-2. Similarly, a contrariety is observed between the results in Fig. 4b). Since the thermal conductivity of C-1 and A-2 grouting materials is fairly identical (Table 3), the temperature decrease at the BHE wall might be equal. Those differences are likely due to the influence of room temperature, because the BHE probe made with C-2 and A-2 materials in dry sand were operated in winter. On the contrary, under water-saturated sand (Fig. 4c) and d)), C-1 and A-2 probes provide nearly similar temperature profile which is in agreement with the fact that they have similar thermal conductivity properties.

The impact of low thermal conductivity of soil can be seen in Fig. 4b) compared to water-saturated sand in Fig. 4d). Close to the BHE probe, the temperature significantly decreased after 50 h operation under dry sand ($\Delta T \sim 6$ K). On the other hand, the heat originated from the BHE propagated further due to better thermal conduction under water-saturated sand that generates lower temperature variation on the BHE wall ($\Delta T \sim 3\text{--}4$ K). Also, under dry sand condition the thermal properties of grouting materials does not have a predominant effect because of the poor thermo-physical properties of the soil in which the main resistance for thermal transfer takes place.

Figs. 5 to 7 compares the temperature distribution in the sandbox over distance and over time with the analytical predictions for operated BHE probe prepared with C-1 silica sand-based grouting, C-2 bentonite-based grouting and A-2 homemade grouting with natural graphite, for dry sand and saturated sand.

Under dry sand condition, a discrepancy can be seen between the analytical solution results and the experimental measurements due to the influence of the boundary conditions (i.e. room temperature) not considered by the analytical solution.

The theoretical results compares fairly well with experimental measurements. It is particularly noticeable, knowing that the analytical results consists in blind prediction (the thermal properties of the different materials have been retrieved from laboratory characterizations and engineering handbooks (Table 2)).

Also, the analytical prediction provides us to cross-check the temperature results which are used to calculate the specific heat extraction rate and the borehole resistance of BHE probes.

In Fig. 8, the specific heat exchange rate and the borehole resistance are deduced from the experimental results according to Eq. (16) and Eq. (15) (Section 4.2.2) and are compared with analytical predictions (Eqs. 1 and 2–10). As demonstrated in Fig. 8, in dry sand, the heat exchange is dominated by the soil thermal characteristics rather than the thermal conductivity of grouting, and the three grouting materials provide similar performance in terms of heat exchange rate. On the other hand, under water-saturated sand condition, C-1 and A-2 exhibit nearly identical performance compared to C-2 bentonite-based grouting due to its lower thermal conductivity. It demonstrates that high thermal properties of grouting materials can be of interest when the thermal conductivity of the ground is sufficiently high.

The heat exchange rates deduced experimentally are fairly well predicted by the analytical solutions. Those predictions were

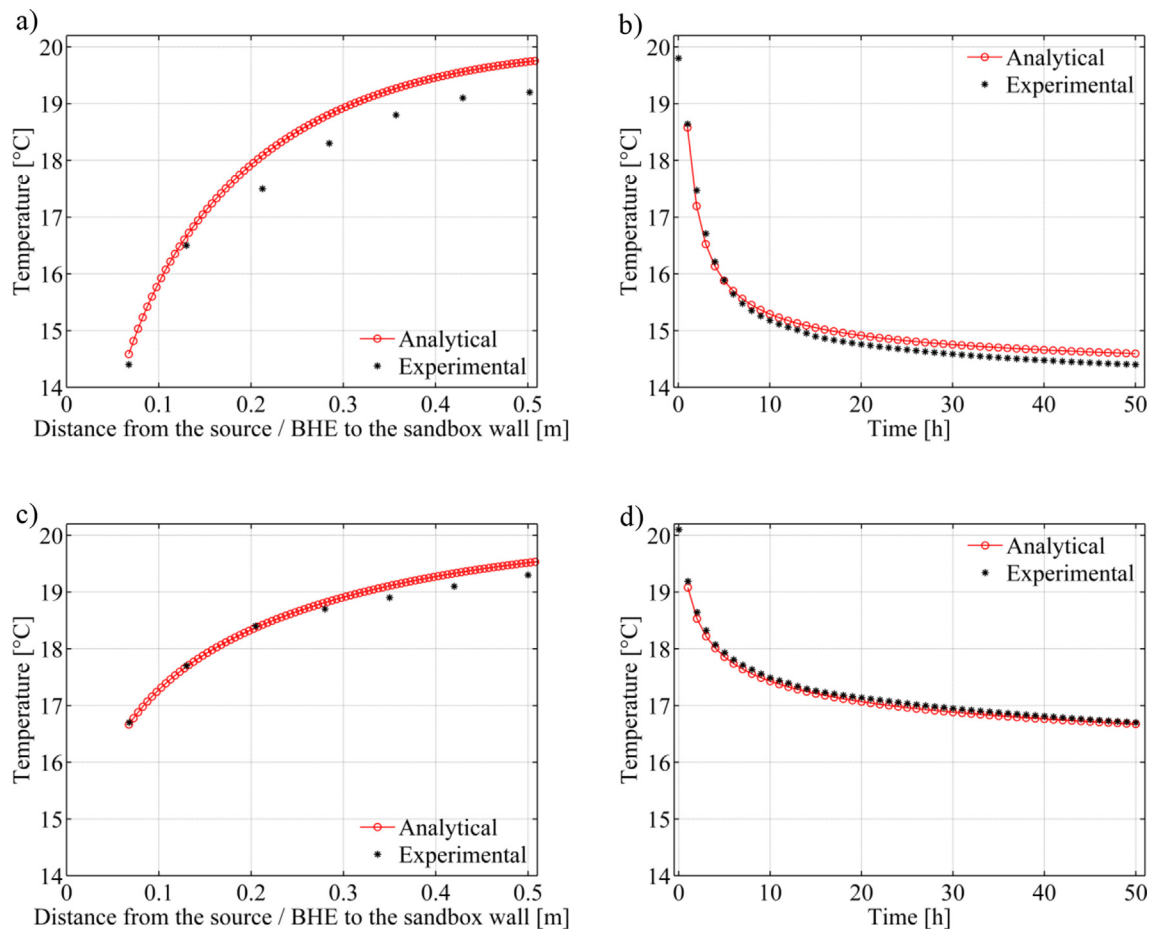


Fig. 6. Comparison of experimental measurement with analytical (Eq. (13)) solution for BHE probe prepared with C-2 bentonite-based grouting: a) and b) dry sand; c) and d) under water-saturated sand. a) and c) at 50th operation hour ($x = 0$ m, $y = 0.068$ m – 0.5 m, $z = 0.5$ m); b) and d) over time ($x = 0$, $y = 0.068$ m, $z = 0.5$ m).

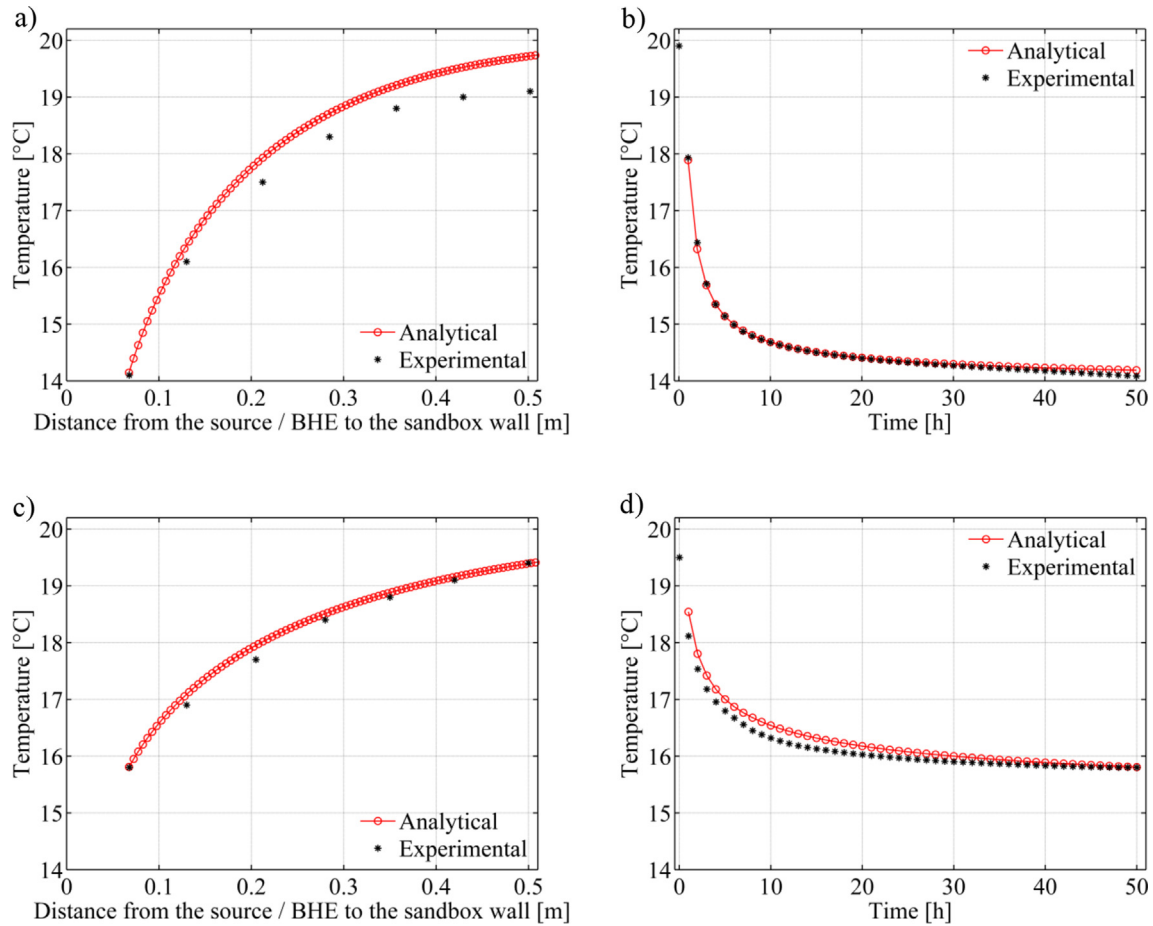


Fig. 7. Comparison of experimental measurement with analytical (Eq. (13)) solution for BHE probe prepared with A-2 homemade with natural graphite: a) and b) dry sand; c) and d) under water-saturated sand. a) and c) at 50th operation hour ($x = 0$ m, $y = 0.068$ m – 0.5 m, $z = 0.5$ m); b) and d) over time ($x = 0$, $y = 0.068$ m, $z = 0.5$ m).

obtained as blind predictions, in the sense that they were deduced from laboratory characterization without any additional adjustments.

As far as the borehole resistances are concerned, since the thermal conductivity of grout is one of the major dependence of the borehole resistance, the mean R_b values of C-1 and A-2 grouting materials shown in Fig. 8b) and d) might be similar (Table 3), as it is obtained experimentally under water saturated sand conditions (Fig. 8d)). In contrast, upon dry sand conditions (Fig. 8b)), the problem of the effect room temperature produces a slight discrepancy in obtained R_b .

6. Conclusion

The grouting material used for BHEs must guarantee several hydraulic, mechanical and thermo-physical requirements. The present study provided a wide investigation on various admixtures including laboratory tests and a comprehensive evaluation of the performance of BHE probes made of different types of grout materials operated in a sandbox.

Thermal, hydraulic and mechanical performance of grouting (bentonite-based material, silica sand-based material and different homemade admixtures with graphite addition) was tested in laboratory. Since the suggestions of existing norms are elusive on the criteria for grout mix of BHEs, the characteristics of different grout mix materials are compared between each other. The Marsh cone test results show that slow efflux time or no-flow condition of

materials may indicate to cause some difficulties during the pumping process of the grouting material, mainly for silica sand-based materials and some homemade admixtures while the flowability of bentonite-based material is much better. Both compression strength and hydraulic permeability of each material show satisfactory results, excepted for the mixture with expanded graphite. In terms of thermo-physical properties, it can be concluded that even a small amount of graphite addition (5%) has a great influence on the thermal conductivity of grout. However, it is not feasible either to increase the fraction of graphite more than 5%, or to use all kind of graphite powders in an admixture used as a backfill material of BHEs, because different specific characteristics of graphite affect adversely the mechanical behaviors of grouts (e.g. flowability, low permeability and compression strength). In fact, the homemade admixture prepared with 5% natural flake graphite can be considered as an appropriate grouting material for BHEs regarding to the laboratory results and the cost aspect. However, this admixture should be tested in real conditions to check if it fulfills the required conditions.

Considering the sandbox results, first, it has been shown that analytical solutions provide good prediction of the observed experimental results, in terms of temperature distribution around the BHE, heat exchange rate and thermal resistance of the BHE. The parameters of the analytical solutions being determined from laboratory characterization, the good matching between the predictions and the measured temperature fields demonstrate that the thermo-physical properties determined at laboratory scale reflect correctly the behavior at the BHE scale.

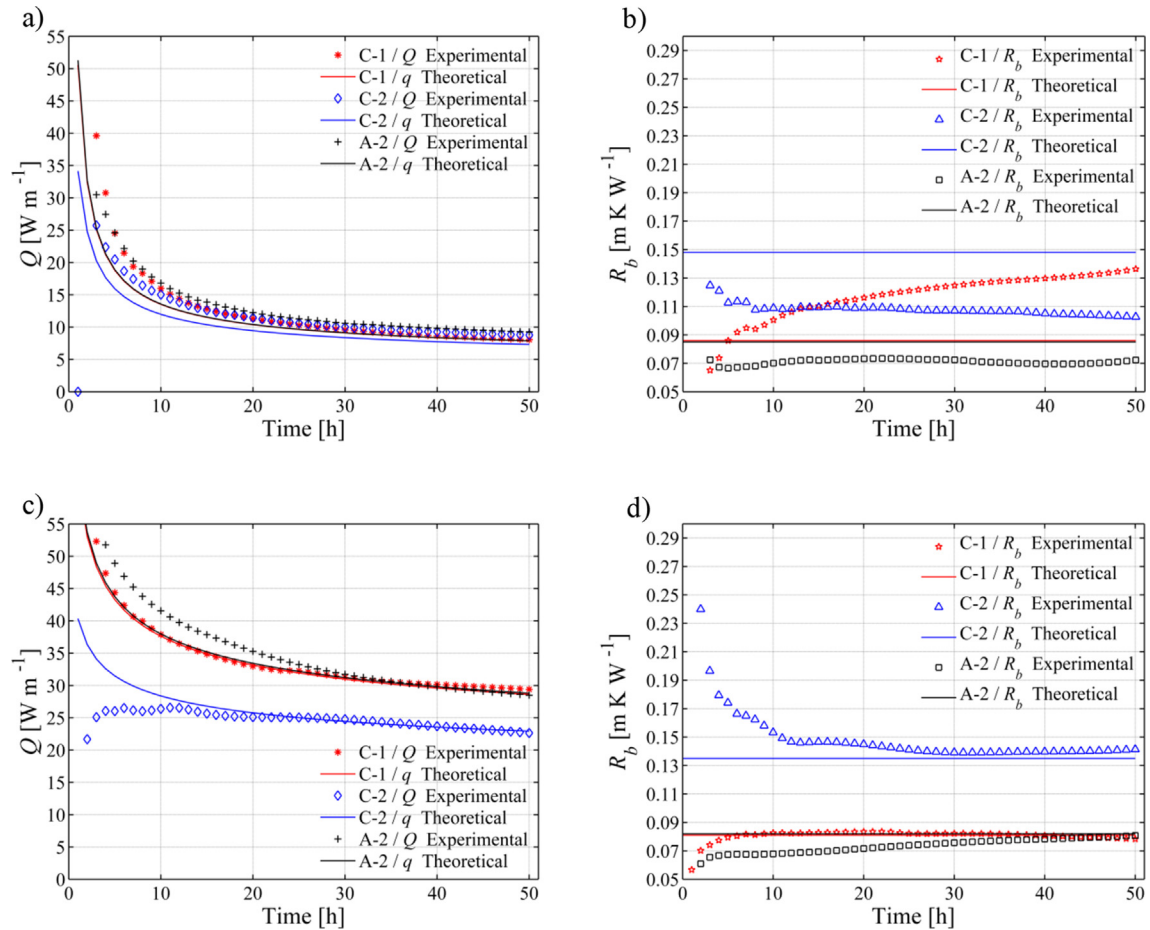


Fig. 8. Comparison the theoretical and the experimental results of specific heat exchange rate (Eq. (1) vs. Eq. (16)) and borehole resistance (Eq. (2) vs. Eq. (15)): Probes operated under a) and b) dry (air – solid) sand; b) and c) water-saturated sand.

If the thermo-physical properties of ground is considerably low (e.g. dry soil), the ground is the main resistance and the thermal conductivity of grout has no significant impact on the specific heat exchange rate. The efficiency of the grout thermal conductivity rises with increasing thermal properties of ground. For the installation of a BHE, the thermal conductivity of ground and backfilling materials may be kept equivalent, high thermo-physical properties of grout being justified only if the conductivity of the ground is high enough.

Acknowledgements

The financial support from Walloon Region in Belgium is profoundly acknowledged (Grant: 1117492 - GeoTherWal - Programme mobilisateur ERable (E24+)). Furthermore, the authors would like to thank the company Schwenk GmbH Germany, Timal Company Switzerland and Sika group Belgium for raw materials. The assistance of Mrs Georgia Ratioti (Université de Liège, Belgium) for the measurement of thermal conductivity of grout is also deeply acknowledged.

References

- [1] M.L. Allan, A.J. Philippopoulos, Thermally Conductive Cementitious Grouts for Geothermal Heat Pumps, 1997. Upton, US-NY: FY 97 Progress Report, BNL 66103.
- [2] M.L. Allan, A.J. Philippopoulos, Properties and Performance of Thermally Conductive Cement-based Grouts for Geothermal Heat Pumps, 1999. Upton, US-NY: FY 99 Final Report, BNL 67006.
- [3] W.A. Austin, C. Yavuzturk, J.D. Spitler, Development of an in-situ system for measuring ground thermal properties, *ASHRAE Trans.* 106 (1) (2000) 365–379.
- [4] J. Bennet, J. Claesson, G. Hellström, Multipole Method to Compute the Conductive Heat Transfer to and between Pipes in a Composite Cylinder, Notes on Heat Transfer 3, Lund Institute of Technology, Lund, Sweden, 1987.
- [5] R. Borinaga-Treviño, P. Pascual-Muñoz, D. Castro-Fresno, E. Blanco-Fernandez, Borehole thermal response and thermal resistance of four different grouting materials measured with a TRT, *Appl. Therm. Eng.* 53 (1) (2013) 13–20.
- [6] H.S. Carslaw, J.C. Jaeger, *Conduction of Heat in Solids*, second ed., Oxford University Press, New York, US-NY, 1959.
- [7] F. Delaleux, X. Py, R. Olives, A. Dominguez, Enhancement of geothermal borehole heat exchangers performances by improvement of bentonite grouts conductivity, *Appl. Therm. Eng.* 33–34 (2012) 92–99.
- [8] J. Desmedt, J. Van Bael, H. Hoes, N. Robeyn, Experimental performance of borehole heat exchangers and grouting materials for ground source heat pumps, *Int. J. Energy Res.* 36 (13) (2012) 1238–1246.
- [9] N. Diao, Q. Li, Z. Fang, Heat transfer in ground heat exchangers with groundwater advection, *Int. J. Therm. Sci.* 43 (12) (2004) 1203–1211.
- [10] S. Erol, M.A. Hashemi, B. François, Analytical solution of discontinuous heat extraction for sustainability and recovery aspects of borehole heat exchangers, *Int. J. Therm. Sci.* (2013) (Submitted).
- [11] Ph.D. Thesis P. Eskilson, Thermal Analysis of Heat Extraction Boreholes, University of Lund, Lund, Sweden, 1987.
- [12] Ph.D. Thesis S. Gehlin, Thermal Response Test – Method, Development and Evaluation, Luleå University of Technology, Luleå, Sweden, 2002.
- [13] S. Gehlin, G. Hellström, Comparison of four models for thermal response test evaluation, *Atlanta, US-GA, ASHRAE Trans.* 109 (1) (2003) 131–142.
- [14] GSHPA, Guideline for Closed Loop Vertical Borehole Heat Exchanger Design, Installation and Material Standards, Ground Source Heat Pump System Association – National Energy Center, Milton Keynes, Buckinghamshire, England, 2011.
- [15] Hakagerodur-geothermal, Handling Book for Borehole Heat Exchangers Technical Details of Geothermal Pipes; Model: Geotherm PE-100, Hakagerodur-geothermal, St. Gallen, Switzerland, 2012. Accessed on March, 12, 2012 by email from Hakagerodur-geothermal AG.

- [16] Ph.D. Thesis G. Hellström, Ground Heat Storage Thermal Analyses of Duct Storage Systems, I. Theory, University of Lund, Lund, Sweden, 1991.
- [17] G. Hellström, Thermal performance of borehole heat exchangers, New Jersey, US-NJ, in: The Second Stockton International Geothermal Conference, 1998.
- [18] Ph.D. Thesis V.J. Herrmann, Ingenieurgeologische Untersuchungen zur Hinterfüllung von Geothermie-Bohrungen mit Erdwärmesonden, Karlsruhe Institute of Technology (KIT), Karlsruhe, Germany, 2008.
- [19] L.R. Ingersoll, O.J. Zobel, A.C. Ingersoll, Heat Conduction with Engineering. Geological and Other Applications, McGraw-Hill, New York, US-NY, 1954.
- [20] M. Jobmann, G. Buntebarth, Influence of graphite and quartz addition on the thermal-physical properties of bentonite for sealing heat-generating radioactive waste, *Appl. Clay Sci.* 44 (2009) 206–210.
- [21] L. Jun, Z. Xu, G. Jun, Y. Jie, Evaluation of heat exchange rate of GHE in geothermal heat pump systems, *Renew. Energy* 34 (12) (2009) 2898–2904.
- [22] L. Lamarche, S. Kaji, B. Beauchamp, A review of methods to evaluate borehole thermal resistances in geothermal heat-pump systems, *Geothermics* 39 (2010) 187–200.
- [23] C. Lee, K. Lee, H. Choi, H.P. Choi, Characteristics of thermally-enhanced bentonite grouts for geothermal heat exchanger in South Korea, *Sci. China Technol. Sci.* 53 (1) (2010) 123–128.
- [24] C. Lee, M. Park, T. Nguyen, B. Sohn, J.M. Choi, H. Choi, Performance evaluation of closed-loop vertical ground heat exchangers by conducting in-situ thermal response tests, *Renew. Energy* 42 (2011) 77–83.
- [25] K. Manohar, D.W. Yarbrough, J.R. Booth, Measurement of apparent thermal conductivity by the thermal probe method, *J. Test. Eval.* 28 (5) (2000) 345–351.
- [26] D. Marcotte, P. Pasquier, F. Sheriff, M. Bernier, The importance of axial effects for borehole design of geothermal heat-pump systems, *Renew. Energy* 35 (4) (2010) 763–770.
- [27] N. Molina-Giraldo, P. Bayer, P. Blum, K. Zhu, Z. Fang, A moving finite line source model to simulate borehole heat exchangers with groundwater advection, *Int. J. Therm. Sci.* 50 (2011) 2506–2513.
- [28] M.Sc. Thesis N.D. Paul, The Effect of Grout Thermal Conductivity on Vertical Geothermal Heat Exchanger Design and Performance, South Dakota University, Vermillion, US-SD, 1996.
- [29] J.P. Remund, J.T. Lund, Thermal enhancement of Bentonite Grouts for Vertical Ground Source Heat Pump Systems, in: AES 29: Heat Pump and Refrigeration Systems, Design, Analysis and Applications H00868–1993, The American Society of Mechanical Engineers (ASME), 1993.
- [30] M. Reuß, M. Proell, R. Koenigsdorff, Quality control of borehole heat exchanger systems, Espoo, Finland, in: IEA ECES Annex 21 Meeting, 2011.
- [31] N. Roussel, R. Le Roy, The Marsh cone: a test or a rheological apparatus? *Cem. Concr. Res.* 35 (5) (2005) 823–830.
- [32] M.H. Sharqawy, E.M. Mokheimer, H.M. Badr, Effective pipe-to-borehole thermal resistance for vertical ground heat exchangers, *Geothermics* 38 (2009) 271–277.
- [33] Sibelco, Handling Book for Silica Sand, Physical Characteristics of Sand M-32 One Grain Size, Sibelco Benelux, Antwerp, Belgium, 2012 (accessed on 07.03.12).
- [34] M.G. Sutton, D.W. Nutter, R.J. Couvillion, A ground resistance for vertical borehole heat exchangers with groundwater flow, *J. Energy Resour. Technol.* 125 (3) (2003) 183–189.
- [35] TIMCAL, Handling Book for Graphite Powder, Technical Data Sheet of TIMREX M100, TIMREX KS150, TIMREX KS 150-600SP and TIMREX C-THERM 01, Graphite & Carbon Manufacturer TIMCAL Ltd., Bodio, Switzerland, 2012 (accessed on 03.07.12).
- [36] VDI-Richtlinie, Thermal Use of the Undergrund – GSHP Systems, VDI 4640 Blatt 2, Verein Deutscher Ingenieure, VDI-Verlag, Düsseldorf, Germany, 2001a.
- [37] VDI-Richtlinie, Utilization of the Subsurface for Thermal Purposes – Underground Thermal Energy Storage, VDI 4640 Blatt 3, Verein Deutscher Ingenieure, VDI-Verlag, Düsseldorf, Germany, 2001b.
- [38] VDI-Richtlinie, Thermal Use of the Undergrund – Direct Uses, VDI 4640 Blatt 4, Verein Deutscher Ingenieure, VDI-Verlag, Düsseldorf, Germany, 2004.
- [39] V. Wagner, P. Bayer, M. Kübert, P. Blum, Numerical sensitivity study of thermal response tests, *Renew. Energy* 41 (2012) 245–253.
- [40] H.Y. Zeng, N.R. Diao, Z.H. Fang, A finite line-source model for boreholes in geothermal heat exchangers, *Heat Transf. Asian Res.* 31 (7) (2002) 558–567.